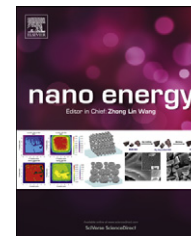


Available online at www.sciencedirect.com

SciVerse ScienceDirect

journal homepage: www.elsevier.com/locate/nanoenergy

RAPID COMMUNICATION

Outstanding performance of activated graphene based supercapacitors in ionic liquid electrolyte from -50 to 80 °C

Wan-Yu Tsai^a, Rongying Lin^a, Shanthi Murali^c, Li Li Zhang^c,
John K. McDonough^d, Rodney S. Ruoff^c, Pierre-Louis Taberna^a,
Yury Gogotsi^{d,*}, Patrice Simon^{a,b,**}

^aUniversité Paul Sabatier, CIRIMAT UMR CNRS 5085, 118 route de Narbonne, 31062 Toulouse, France

^bRéseau sur le Stockage Electrochimique de l'Energie (RS2E), FR CNRS 3459, France

^cDepartment of Mechanical Engineering and the Materials Science and Engineering Program, The University of Texas at Austin, One University Station C2200, Austin, TX 78712, United States

^dDepartment of Materials Science and Engineering & A.J. Drexel Nanotechnology Institute, Drexel University, 3141 Chestnut St., Philadelphia, PA 19104, United States

Received 8 October 2012; received in revised form 7 November 2012; accepted 12 November 2012

KEYWORDS

Electrochemical capacitors;
Activated graphene;
Ionic liquid mixture;
Wide temperature range

Abstract

High specific surface area (SSA ~ 2000 m²/g) porous KOH-activated microwave exfoliated graphite oxide ('a-MEGO') electrodes have been tested in a eutectic mixture of ionic liquids (1:1 by weight or molar ratio N-methyl-N-propylpiperidinium bis(fluorosulfonyl)imide (PIP₁₃-FSI) and N-butyl-N-methylpyrrolidinium bis(fluorosulfonyl)imide (PYR₁₄-FSI)) as electrolyte for supercapacitor applications. By optimizing the carbon/electrolyte system, outstanding capacitive performance has been achieved with high capacitance (up to 180 F/g) and wide electrochemical window (up to 3.5 V) over a wide temperature range from -50 °C to 80 °C. This is the first demonstration of a carbon-ionic liquid system capable of delivering capacitance in excess of 100 F/g below room temperature. The excellent electrochemical response of the proposed couple shows that optimization of the carbon/electrolyte interface is of great importance for improving capacitive energy storage.

© 2012 Elsevier Ltd. All rights reserved.

Introduction

Electrochemical double layer capacitors (EDLCs), also known as supercapacitors, store electrical charges between electrode materials and electrolyte ions by electrostatic

*Corresponding author. Tel.: +1 215 895 6446.

**Corresponding author. Tel: +33 5 615 568 02

E-mail addresses: simon@chimie.ups-tlse.fr (P. Simon), Gogotsi@drexel.edu (Y. Gogotsi).

attractions. Supercapacitors had their debut mainly in CMOS memory back-up and are now widely used in power electronics for peak power shaving and back-up supplies (as support for power disruption). Today, one of the most promising applications is their use in transportation (in hybrid-electric vehicles (HEVs) in particular) for harvesting braking energy and for faster start-up of the engine [1-3]. Their increasing use for energy storage is due to a number of factors including (i) their high power densities (>10 kW/kg), (ii) moderate energy density (~ 5 -6 Wh/kg), (iii) that they can be fully charged/discharged in a matter of seconds [4,5], (iv) the cost competitiveness of the materials that they are comprised of, (v) high charge/discharge efficiency, and (vi) their high cycle life, which is generally longer than the life of the device being powered.

Generally, EDLCs are made up of two symmetrical activated carbon electrodes that display symmetric charge/discharge power capability over the complete range of potential operation (i.e., from the maximum rated voltage to near zero). Carbon/carbon supercapacitors can be used over the complete voltage range without damage for at least 1 million cycles [6]. Carbon-based electrodes are of great interest because they are light, of moderate cost, abundant, easy to process, and possess high electronic conductivity and high specific surface area (yielding high charge storage). A variety of different carbon nanostructures can be produced that have very high surface areas and a wide variety of physical properties, which allows targeting of different types of applications. Templated carbons [7], carbide-derived carbons (CDCs) [8-10], 'onion-like' carbons (OLCs) [11], carbon fabrics (cloth, fibers) [12], nanotubes [13], activated graphene [14] and nanohorns [15] have been used as electrodes for EDLC applications [16].

Batteries have much higher energy densities (up to 250 Wh/kg for Li-ion) than current commercial supercapacitors (5 Wh/kg) [17]. One approach to increase energy density of supercapacitors is with ionic liquid electrolytes that offer better electrochemical stability than that of the aqueous (1.23 V) and organic (2.7 V) electrolytes currently used. Ionic liquids (IL) - salts (mainly, organic) that are liquid at room temperature - are being explored as electrolytes for Electrical Energy Storage (EES) systems owing to their high thermal (up to 350 °C) and electrochemical (up to 6 V) stability [18]. Their high heat capacity, a large cohesive energy, and negligible vapor pressure at elevated temperatures make them safe and non-flammable electrolytes. This is especially important in energy storage applications when devices need to perform under extreme temperature conditions that can raise/cause safety issues. The *raison d'être* for exploring eutectic mixtures of ionic liquids is their large stable liquidus temperature range (the span of temperatures between the freezing point and boiling point of a liquid, such as from -80 °C to ≥ 250 °C). The size and symmetry of cations strongly influence the melting points of ionic liquids. Usually, one of the two pairing ions (usually the cation) is particularly large and possesses a low degree of symmetry, leading to inefficient packing of the large irregular cations with small charge-delocalized anions, which is why organic salts have a reduced crystal lattice energy and hence a lower melting point compared to inorganic salts [19]. Binary and ternary eutectic mixtures have been studied for EES systems. Binary eutectic systems

first appeared with the discovery by Wilkes et al. in 1982 of a MeEtImCl/AlCl₃ molten salt mixture that was liquid over a wide range of compositions and to temperatures as low as -98 °C for a composition of 67% AlCl₃ [20]. Other binary systems have been investigated by Hou et al. [21] using imidazolium-based ILs with organic salts. Every et al. [22] reported a eutectic mixture of pure ILs (mixing ethylmethyl-imidazolium tri-fluorosulfonyl-imide (EMI-TFSI) and EMI-CF₃SO₃⁻ (triflate)) with no evidence of a melting point, indeed only a glass transition was observed. Pyrrolidinium-based mixtures with TFSI-FSI-based ILs were also found by differential scanning calorimetry to form eutectic mixtures [23]. Deeper eutectics (-95 °C) were however observed to be mainly in mixtures of a common cation with two different anions compared to eutectics (-25 °C) in mixtures of a common anion with two different cations. Other binary systems include IL-LiX mixtures as electrolytes for battery applications [24-26]. Henderson et al. [24] reported decreasing the eutectic temperatures of pyrrolidinium-based ILs by using different alkyl chain lengths and Li salt concentrations.

As reported before, we have designed IL mixtures with exactly the same anion (FSI) but two different cations: piperidinium (PIP) and pyrrolidinium (PYR) [27]. These cations have the same molecular weight and the same number of atoms of the same nature, with the only difference being their cation molecular structure, namely a five-member (piperidinium) or six-member (pyrrolidinium) heterocycle. Methyl+propyl substituent groups (total of 4 carbons on side chains) are used for synthesizing the PIP-based cation and methyl+butyl substituent groups (total of 5 carbons on side chains) for synthesizing the PYR-based cation. The concept is to maintain similar intermolecular interactions due to the similar constituent atoms of the two cations, while also increasing disorder and asymmetry among the cations to hinder lattice formation to lower the melting point, but still maintaining good miscibility. Amongst common anions such as hexafluorophosphate (PF₆⁻), tetrafluoroborate (BF₄⁻), bis(trifluorosulfonyl)imide (TFSI⁻) and bis(fluorosulfonyl)imide (FSI⁻) anions, the imides (TFSI⁻ and FSI⁻) have emerged as popular alternatives to the PF₆⁻ and BF₄⁻ anions due to the susceptibility of the PF₆⁻ and BF₄⁻ anions to hydrolysis, leading to the production of hazardous hydrogen fluoride [28-32]. This is why hydrophobic TFSI⁻ and FSI⁻ anions are increasingly being studied as electrolytes for energy storage [33-35]. The FSI⁻ ion has been selected to be the anion for the electrolyte used in this study due to its generally higher conductivity and lower viscosity as compared to the TFSI⁻ ion when paired with the same cation [36], because of the smaller size and hence higher mobility of the FSI⁻ ion. Cations were chosen by comparing their stability. The electrochemical stability of commonly used cations of ILs decreases in the order of Ammonium \approx Piperidinium \geq Pyrrolidinium $>$ Imidazolium [37]. Hence, cations with functional groups of pyrrolidinium (PYR) and piperidinium (PIP) with relatively higher electrochemical stability were explored.

A eutectic mixture composed of (1:1 by weight or molar ratio) N-methyl-N-propylpiperidinium bis(fluorosulfonyl)imide (PIP₁₃-FSI) and N-butyl-N-methylpyrrolidinium bis(fluorosulfonyl)imide (PYR₁₄-FSI) was prepared and used as electrolyte. The measured melting points of constituents of this IL mixture were 6 °C (PIP₁₃-FSI) and -18 °C (PYR₁₄-FSI), in good agreement with

published data [23]. The liquid state of this IL eutectic mixture can be maintained at temperatures several tens of degrees lower compared to the individual ILs. Mixing PIP₁₃-FSI with PYR₁₄-FSI resulted in an IL with two different cationic species and only one anion (namely, (PIP₁₃-FSI)_{0.5}(PYR₁₄-FSI)_{0.5}), which expands the liquid range to $-80\text{ }^{\circ}\text{C}$ as reported previously [27]. Most importantly, the wide electrochemical stability window is preserved in the mixtures, which contributes to the goal of increasing energy density, as $E = \frac{1}{2}CV^2$, where C is capacitance and V is voltage. This electrolyte mixture was used in our previous work with nanostructured carbon electrodes of either onion-like carbon (OLC) or carbon nanotubes (CNTs) [27]. Excellent capacitive behavior has been observed in an extended operating temperature range of $-50\text{ }^{\circ}\text{C}$ to $100\text{ }^{\circ}\text{C}$. However, the specific capacitance obtained in these exohedral carbons was low ($\sim 30\text{ F/g}$; 4 mF/cm^2), because of their moderate SSA and highly graphitic surface. This suggests increasing SSA and improving the carbon/electrolyte interface to increase the magnitude and quality of charge storage, thereby further improving the energy density and in an extended operating temperature range. However, nanoporous activated or carbide-derived carbons that possess a high SSA and show excellent performance in organic electrolytes, show poor capacitive performance with IL electrolytes at room temperature or below [10,27,34] due to low mobility of ions in porous networks. To the best of our knowledge, no carbon electrode material has ever shown capacitance of 100 F/g or higher in any IL electrolyte below room temperature.

Ruoff's group recently reported on the activation of microwave exfoliated graphite oxide ('a-MEGO') using potassium hydroxide [38]. This carbon ('a-MEGO') had unique structure and properties, such as high SSA, approaching and even exceeding that of single-layer graphene, as measured by the Brunauer-Emmett-Teller (BET) method [39], along with a continuous, three dimensional pore structure consisting of atom-thick walls and both micro- and mesopores. It showed high capacitance in IL electrolyte at room temperature, but has not been tested at low temperatures. Since a-MEGO possesses high electrical conductivity, low O and H content, and is composed mostly of sp^2 bonded carbon, we reasoned that it might yield a dramatic increase in specific capacitance, compared to OLC or CNTs, with the (PIP₁₃-FSI)_{0.5}(PYR₁₄-FSI)_{0.5} ionic liquid electrolyte.

Experimental

The synthesis procedure for a-MEGO, as well as its structure, has been described in Ref. [38]. MEGO was prepared from graphite oxide (GO) by microwave irradiation [40], then dispersed and soaked in aqueous KOH solution for 20 h. The solid cake obtained after vacuum filtration of the excess KOH was then dried. The dry MEGO/KOH mixture was heated at $800\text{ }^{\circ}\text{C}$ for 1 h in a horizontal tube furnace with an argon flow of 150 sccm at atmospheric pressure. The sample was then washed with de-ionized water, and dried at $65\text{ }^{\circ}\text{C}$ in ambient air for 2 h. Annealing of activated graphene was done in a custom made vacuum furnace (Solar Atmospheres, USA) at $1100\text{ }^{\circ}\text{C}$, with the heating ramp $10\text{ }^{\circ}\text{C/min}$, and a vacuum $\sim 10^{-6}$ Torr for 10 min.

Nitrogen gas sorption was performed at 77 K using a Quadrasorb Pore Size and Surface Area Analyzer

(Quantachrome Instruments, USA). Prior to analysis, samples were outgassed at $200\text{ }^{\circ}\text{C}$ in vacuum at about 10^{-2} Torr for 24 h. Surface area was calculated using the BET method in the range of $0.05\text{--}0.3P/P_0$. Pore size distributions (PSD) were determined using the quenched solid density functional theory (QSDFT) model, assuming a slit pore geometry, which was part of the QuadraWin software package (Quantachrome Instruments, USA).

Raman spectra were recorded with an Invia confocal Raman spectrometer (Renishaw, UK) using a laser with an excitation wavelength of 514.5 nm and having a spot size of $2\text{ }\mu\text{m}$.

ILs were prepared at Solvionic SA (France). N-methyl-N-butylpyrrolidinium bromide, PYR₁₄-Br, is first produced from the quaternization of methyl-pyrrolidine by 1-bromobutane to yield its halide salt, PYR₁₄-Br. The desired PYR₁₄-FSI IL was then obtained through the anionic exchange of the Br⁻ with potassium bis(fluorosulfonyl)imide (KFSI). N-methyl-N-propylpiperidinium bromide, PIP₁₃-Br, was obtained from the quaternization of N-methyl-N-propylpiperidine by 1-bromopropane to yield its halide salt, PIP₁₃-Br and the subsequent metathesis (with KFSI) to obtain the product PIP₁₃-FSI. The eutectic IL mixture (1:1 by weight) was then obtained by mixing N-methyl-N-propylpiperidinium bis(fluorosulfonyl)imide (PIP₁₃FSI) and N-butyl-N-methylpyrrolidinium bis(fluorosulfonyl)imide (PYR₁₄FSI) [27].

Microcavity electrode measurements that have been described in our previous work [11,41] were done on the a-MEGO powders under glovebox conditions of $<0.1\text{ ppm}$ of water and oxygen content. A two-electrode Swagelok[®] nylon cell with stainless steel pistons was used for quantitative electrochemical characterizations of as-activated MEGO (i.e., a-MEGO) powders, and a three-electrode Swagelok[®] nylon cell was used to characterize vacuum annealed a-MEGO powders. Each cell was assembled in the eutectic mixture of ILs under glove-box conditions. Pt disks were placed onto stainless steel current collectors to decrease the contact resistance at the as-activated a-MEGO/piston interface. A silver wire was used as a quasi-reference electrode. The as-activated a-MEGO, electrode films (disks) of 1.1 cm^2 , 1.65 mg , and $55\text{ }\mu\text{m}$ thick were made of 95% of the carbon powder and 5% of PTFE (Dupont de Nemours) binder as described in Zhu et al. [38], whereas for the annealed a-MEGO, the powder was tested directly without film processing. Electrodes were wetted with the electrolyte and covered by two layers of $25\text{ }\mu\text{m}$ -thick porous Al₂O₃ separator (Separion[®], average pore size of 240 nm , $>40\%$ porosity, Evonik Industries, Germany); these separators were wetted by the electrolyte prior to being placed between the electrodes. Swagelok[®] cells were kept under light pressure during the measurement to buffer thermal expansion/contraction of the stainless steel pistons. Temperature control was achieved using a Votsch climatic chamber (Germany) with the temperature being additionally checked by a thermocouple. After heating to a certain temperature, the system was kept isothermal for a period of no less than 5 h prior to electrochemical measurements to ensure system equilibration. For low temperature experiments, this dwell time was increased to an overnight period ($>6\text{ h}$).

Capacitance was calculated from cyclic voltammetry (CV) by measuring the slope of a charge Q versus voltage (V) plot. Charge was calculated from the integration of the area under the voltammogram obtained in discharge.

The current in the CVs in Figs. 3a, 4a, c, and 5b was normalized by dividing the current values by the potential scan rate to obtain capacitance (C).

Results and discussion

Single-layer graphene has a theoretical specific surface area of $2630 \text{ m}^2/\text{g}$ however in practice the BET SSA is generally much lower because of multi-layer sheets and agglomeration. We approach the theoretical value of a single sheet of graphene, with as-activated a-MEGO having a high surface area of $1901 \text{ m}^2/\text{g}$ and all pores less than 5 nm (Figure 1a). The a-MEGO was vacuum annealed at $1100 \text{ }^\circ\text{C}$ in an attempt to remove the oxygen containing surface functional groups. At this temperature (and for the 'right' exposure time), one might expect that oxygen containing groups would be removed while the structure of the a-MEGO might be preserved. From Figure 1b, after annealing, the BET SSA is $1586 \text{ m}^2/\text{g}$, and the peak in the PSD around 3.25 nm is smaller than that of the as-activated a-MEGO. The microporous region ($<2 \text{ nm}$) was unchanged after annealing, indicating the initial pore structure in a-MEGO has been largely preserved. The vacuum annealed a-MEGO has a desirable PSD for supercapacitors, as it has both micropores that give it a high SSA, in the range of values typical for activated carbons, and mesopores that facilitate ion mobility during charging and discharging.

Comparing the pore structure of vacuum annealed a-MEGO to the as-activated a-MEGO material that was recently reported and tested in supercapacitors at room temperature [38], the pore size distribution of the vacuum annealed a-MEGO made here tends to a smaller average pore size and a smaller specific surface area, with the previously reported a-MEGO having a 'high end' value of BET SSA of $\sim 3100 \text{ m}^2/\text{g}$ [38]. Both materials have all pores less than 10 nm . Other materials for supercapacitors, such as CDC and activated carbon, have similar surface areas to vacuum annealed a-MEGO, but tend to have an intricate network of pores that limits ion transport rates and prevents fast charging and discharging when viscous IL electrolytes are used [27,34].

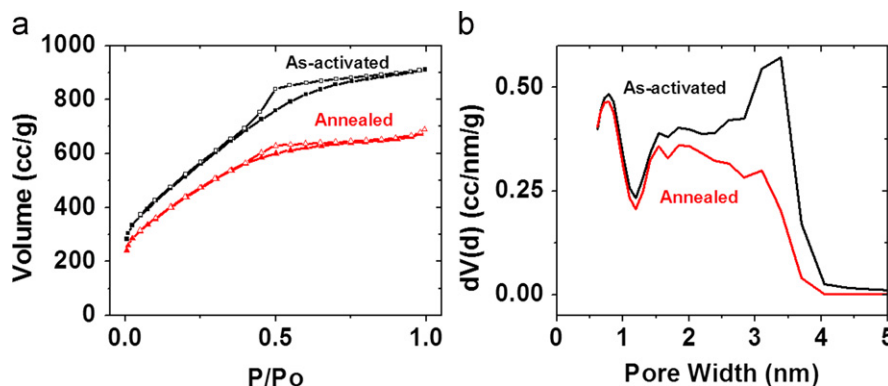


Figure 1 Nitrogen sorption isotherms (a) and corresponding pore size distributions (b) for as-activated (BET SSA $1900 \text{ m}^2/\text{g}$) and vacuum annealed a-MEGO (BET SSA $1590 \text{ m}^2/\text{g}$). After annealing, there is a decrease in the volume of small mesopores around 3 nm , while the micropores within a-MEGO are preserved. Closed symbols in (a) represent the adsorption branch while open symbols represent the desorption branch.

The disorder and graphitic nature of the structure before and after annealing was analyzed using Raman spectroscopy (Figure 2). There is very little difference in the two spectra, implying the annealing process did not change the graphene layer structure. The main difference lies in the full width at half maximum (FWHM) of the disorder-induced (D) band, which narrows after annealing from 160 to 140 cm^{-1} , implying healing of some defects. The main goal of annealing the a-MEGO was to remove oxygen groups on the surface without affecting a-MEGO structure, which seems to be successful from the Raman spectra as the difference before and after annealing is subtle.

Figure 3a shows the CV scanned at 20 mV/s at room temperature of the as-activated a-MEGO electrodes in the IL mixture presented in terms of capacitance versus voltage of the cell. This again confirms the feasibility of using the eutectic IL mixture with as-activated a-MEGO and annealed a-MEGO, in addition to the previous OLCs and CNTs [27] that have been tested. A maximum operating voltage of 3.5 V (same as for the OLCs) [27] was obtained at room temperature with a capacitance of $\sim 160 \text{ F/g}$, a 5-fold increase compared to

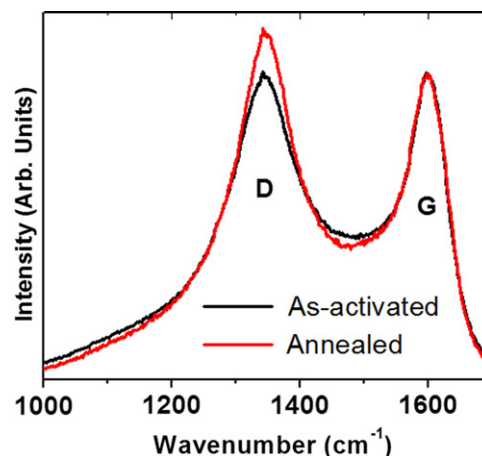


Figure 2 Raman spectra of as-a-MEGO in the carbon spectral range showing the bands corresponding to disordered structures (D) around 1350 cm^{-1} and in-plane vibrations of graphite (G) around 1600 cm^{-1} . Note that there is no significant change of the structure as a result of annealing.

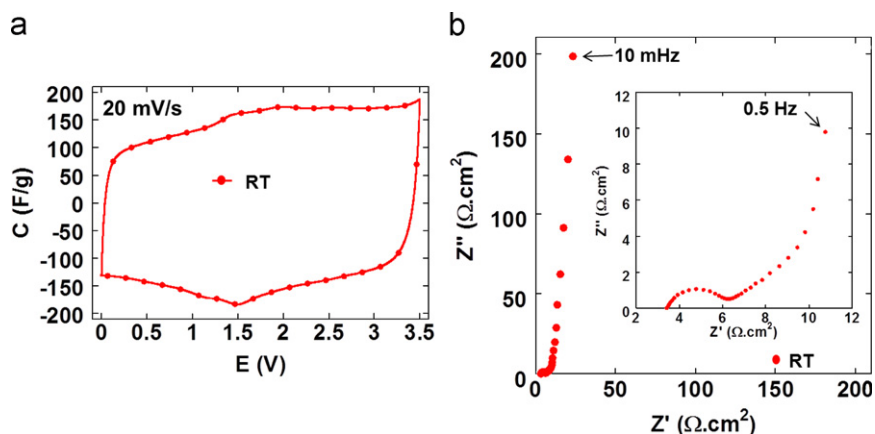


Figure 3 Room temperature electrochemical characterization of a-MEGO electrodes in $(\text{PIP}_{13}\text{-FSI})_{0.5}(\text{PYR}_{14}\text{-FSI})_{0.5}$ electrolyte: CVs collected at 20 mV/s with the electrochemical window of 3.5 V and showing capacitance of 150 F/g (a) and the corresponding EIS Nyquist plot (b). Inset in (b) shows data at the high-frequency range.

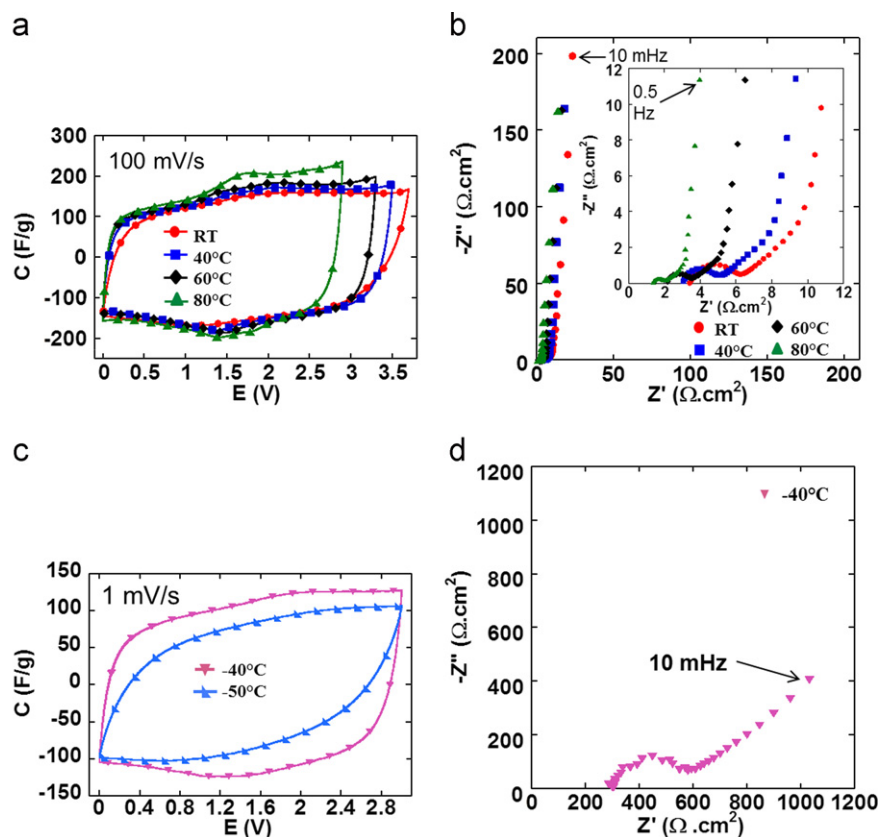


Figure 4 Electrochemical characterization of a-MEGO electrodes in $(\text{PIP}_{13}\text{-FSI})_{0.5}(\text{PYR}_{14}\text{-FSI})_{0.5}$ electrolyte: CVs collected at 100 mV/s (a), corresponding EIS Nyquist plots (b) at room and elevated temperatures ($\text{RT} \leq T \leq 80^\circ\text{C}$), and CVs collected at 1 mV/s ($T \leq -40^\circ\text{C}$) (c) and the corresponding EIS Nyquist plot at $T = -40^\circ\text{C}$ (d).

OLCs and CNTs (~ 30 F/g) [27]. This huge increase can be firstly attributed to the SSA of the as-activated a-MEGO electrodes, which is at least 4 times larger than that of OLC (~ 400 m²/g). Moreover, the open inter-layer porosity (up to 4 nm) of the as-activated a-MEGO electrodes allows electrolyte ions access to the subnanometer pores in a-MEGO sheets without much limitation in ion transfer, as may occur when using conventional

activated carbons with a tortuous pore network and narrow bottlenecks between pores [27].

Figure 3b shows the EIS plot for the a-MEGO electrodes assembled in the ionic liquid mixture. The vertical increase of the imaginary part of the impedance provides evidence of the capacitive storage achieved with a-MEGO. A fairly low ESR of $3.4 \Omega \text{ cm}^2$ (intercept of the X-axis at high frequency)

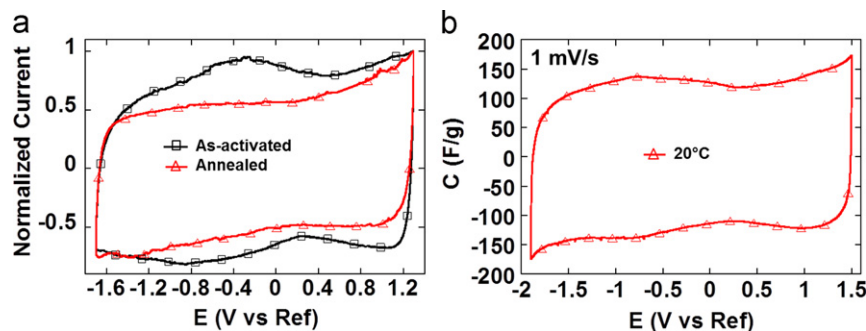


Figure 5 Cyclic voltammograms of annealed and as-activated a-MEGO electrodes in $(\text{PIP}_{13}\text{-FSI})_{0.5}(\text{PYR}_{14}\text{-FSI})_{0.5}$ electrolyte: CVs collected at 500 mV/s at room temperature using CME (a); CV collected at 1 mV/s using a Swagelok[®] cell (b).

was measured at room temperature ($10 \Omega \text{ cm}^2$ ESR was measured for CNT electrodes [27]), mainly due to the high electrical conductivity of the a-MEGO electrode (500 S/cm) compared to commercial activated carbons (0.1-1 S/cm) [42]. Since both sides of the atom-thick pore walls of a-MEGO (graphene-like layers) can be used in charge storage, once the electrolyte gains access to these surfaces, a tremendous amount of charge could be stored as observed in the 5-fold increase in capacitance using a-MEGO instead of OLCs. This capacitance value is in agreement with the value reported by Zhu et al. [38] using neat EMI-TFSI with as-activated a-MEGO electrodes.

Capacitance at Elevated Temperature ($20 \leq T \leq 80 \text{ }^\circ\text{C}$): Figure 4a shows CVs recorded at 100 mV/s to their respective maximum voltages at different temperatures. There is a gradual increase of capacitance (area under the CV curve) with increasing temperature that can be explained by the higher ionic conductivity (ion mobility) of the electrolyte at elevated temperatures, which is also reflected in the more rectangular shape of the CVs with increasing temperature. Electrochemical impedance measurements further confirm the decrease in ionic resistance as shown in Figure 4b and the ESR value decreases from 3.4 to $1.3 \Omega \text{ cm}^2$ upon increasing the temperature from 20 $^\circ\text{C}$ to 80 $^\circ\text{C}$. The capacitance increases from 160 to 180 F/g as temperature increases from RT to 80 $^\circ\text{C}$. The operating voltage is limited to 2.9 V at 80 $^\circ\text{C}$, which is linked with the enhanced electrolyte electrochemical activity at platinum current collectors at elevated temperature (see Supplementary Figure S1).

Capacitance at sub-zero temperatures (-40 and $-50 \text{ }^\circ\text{C}$): Figure 4c shows the CVs recorded at sub-zero temperatures of -40 and $-50 \text{ }^\circ\text{C}$. About 70% of the capacitance is still retained at 1 mV/s (which is a reasonable scan rate taking into account the reduced ion mobility for such low temperatures) and the CVs show good capacitive behavior at $-40 \text{ }^\circ\text{C}$ with high capacitance values of 100 to 120 F/g obtained when charged to 3 V. Such retention of capacitance over this wide operating temperature range (from $-50 \text{ }^\circ\text{C}$ to 80 $^\circ\text{C}$) with capacitance always above 100 F/g, to our knowledge, has never been reported before in the literature [43-48]. EIS measurements still show a capacitive behavior, despite the presence of an expected extra semi-circle at high frequency, attributed to the onset of gelation that is related to decreased mobility of the electrolyte ions within the pores of a-MEGO at such low temperatures

Table 1 Capacitance of annealed a-MEGO electrodes in $(\text{PIP}_{13}\text{-FSI})_{0.5}(\text{PYR}_{14}\text{-FSI})_{0.5}$ electrolyte at room temperature.

Scan rate (mV/s)	Charging/discharging capacitance (F/g)
20	100
5	110
1	130

[49-51]. The capacitive behavior of a-MEGO decreases at $-50 \text{ }^\circ\text{C}$ which is evident by a less rectangular CV than that seen in the CNTs.

While the a-MEGO electrodes show outstanding capacitance of $\sim 180 \text{ F/g}$ (see Figure 3a), the presence of bumps in the CV at about 1.5 V could be due to electrochemically active oxygen-containing functional groups, such as carboxylic acid or hydroxyl groups on their surface. Such bumps were also observed when a-MEGO electrodes were tested in EMI-TFSI electrolyte [38]. Although they are suitable for improving the capacitance, such surface groups are known to be unstable during cycling, thus limiting the cycle life of the cells [16]. This motivated annealing a-MEGO powder at 1100 $^\circ\text{C}$ under vacuum to try to eliminate functional groups that may be present on its surface. Annealed and as-activated a-MEGO powders were tested in the eutectic IL mixture at room temperature using a microcavity electrode to obtain information on any difference in electrochemical response as a result of vacuum annealing. The CVs collected from both samples in a 3-electrode cell are shown in Figure 5a, scanned within a potential window of -1.7 to 1.3 V/Ref. Bumps observed at $\sim -0.3 \text{ V/Ref}$ in the positive scan and at $\sim -0.8 \text{ V/Ref}$ in the negative scan are pronounced for the as-activated a-MEGO powder and clearly decreased after annealing.

Annealed a-MEGO powders were then characterized in Swagelok[®] cells, using a 3-electrode configuration. Figure 5b shows the CV of annealed a-MEGO powders at 1 mV/s at room temperature. Note that in these experiments, raw powders were tested without any binder so that the ohmic drop was not optimized in the cell which is why a low scan rate was used. Annealed a-MEGO powders reached a capacitance of 130 F/g, which is $\sim 20\%$ less than the

capacitance obtained for the as-activated samples, as expected from a lower SSA of the annealed material. The other point to be taken into account is the processing of the electrode, which could have some effect on capacitance values measured (Figure 5b). In conclusion, the high capacitance of the a-MEGO materials observed in the ionic liquid mixture can be primarily associated with double layer charging as shown in Table 1.

Conclusions

The electrochemical characterization of as-activated and vacuum annealed a-MEGO has been carried out in a eutectic mixture of ionic liquids, (PIP₁₃-FSI)_{0.5}(PYR₁₄-FSI)_{0.5}. Annealing the a-MEGO yields better electrochemical stability, but the specific capacitance somewhat decreases due to decreased mesoporosity and associated accessible SSA after annealing.

For ionic liquid electrolytes, an exceptionally high capacitance of about 150 F/g, with a maximum voltage of 3.5 V was attained over an unprecedented 130 °C (from –50 to 80 °C) temperature window. This is 5 times higher capacitance compared to exohedral nanostructured carbon (nanotubes and onions) electrodes in the same eutectic mixture of ionic liquids. These findings have largely overcast the temperature range offered by conventional organic electrolytes of 110 °C (from –30 °C to 80 °C) and would greatly contribute to the advances in electrical storage based on ILs, pushing the limits of energy storage to greater heights. These studies have not only affirmed our previous findings on the need to design carbon structure for optimizing carbon/electrolyte interface, but also showed that ionic liquids are no longer confined to the category of “above room temperature” applications. Even more, they have proved their extended threshold for extreme climatic conditions, which clearly proves the robustness of ILs as electrolytes for electrical storage.

Herein, the research pathway has been paved towards optimizing the carbon accessible surface area (e.g., by using activated graphene, i.e., a-MEGO [38], de-bundled single-walled nanotubes [52], or mesoporous templated carbons [53]) together with designing the IL-based electrolyte. Control of the electrolyte composition and its molecular/ionic structure is required for achieving better compatibilities with various carbon structures and surpassing the current capacitance and energy density limits of EES.

Acknowledgments

P. Simon would like to thank the European Research Council for supporting the research (Advanced Grant no. ERC-2011-AdG, Project no. 291543 - IONACES); W.-Y. Tsai was fully supported by the ERC Grant. Y. Gogotsi and J. McDonough were supported as part of the Fluid Interface Reactions, Structures and Transport (FIRST) Center, an Energy Frontier Research Center funded by the US Department of Energy, Office of Science, Office of Basic Energy Sciences. Work at UT Austin was supported by the US Department of Energy (DOE) under Award no. DE-SC001951.

Appendix A. Supporting information

Supplementary data associated with this article can be found in the online version at <http://dx.doi.org/10.1016/j.nanoen.2012.11.006>.

References

- [1] R. Kotz, M. Carlen, *Electrochimica Acta* 45 (2000) 2483-2498.
- [2] A. Burke, *Journal of Power Sources* 91 (2000) 37-50.
- [3] R.J. Brodd, K.R. Bullock, R.A. Leising, R.L. Middaugh, J.R. Miller, E. Takeuchi, *Journal of the Electrochemical Society* 151 (2004) K1-K11.
- [4] J.R. Miller, P. Simon, *Science* 321 (2008) 651-652.
- [5] P. Simon, Y. Gogotsi, *Nature Materials* 7 (2008) 845-854.
- [6] M. Everett, *Ultracapacitors: a mature energy-storage alternative in a dramatically expanding application set*, Maxwell Technologies, in: *Proceedings of the AABC Conference*, Mainz, Germany, June 18-22, 2012.
- [7] A. Kajdos, A. Kvit, F. Jones, J. Jagiello, G. Yushin, *Journal of the American Chemical Society* 132 (2010) 3252-3253.
- [8] A. Janes, E. Lust, *Journal of the Electrochemical Society* 153 (2006) A113-A116.
- [9] B.D. Shanina, A.A. Konchits, S.P. Kolesnik, A.I. Veynger, A.M. Danishevskii, V.V. Popov, S.K. Gordeev, A.V. Grechinskaya, *Carbon* 41 (2003) 3027-3036.
- [10] V. Presser, M. Heon, Y. Gogotsi, *Advanced Functional Materials* 21 (2011) 810-833.
- [11] C. Portet, J. Chmiola, Y. Gogotsi, S. Park, K. Lian, *Electrochimica Acta* 53 (2008) 7675-7680.
- [12] K. Okajima, K. Ohta, M. Sudoh, *Electrochimica Acta* 50 (2005) 2227-2231.
- [13] D.N. Futaba, K. Hata, T. Yamada, T. Hiraoka, Y. Hayamizu, Y. Kakudate, O. Tanaike, H. Hatori, M. Yumura, S. Iijima, *Nature Materials* 5 (2006) 987-994.
- [14] M.D. Stoller, S. Park, Y. Zhu, J. An, R.S. Ruoff, *Nano Letters* 8 (2008) 3498-3502.
- [15] C.-M. Yang, Y.-J. Kim, M. Endo, H. Kanoh, M. Yudasaka, S. Iijima, K. Kaneko, *Journal of the American Chemical Society* 129 (2007) 20-21.
- [16] A.G. Pandolfo, A.F. Hollenkamp, *Journal of Power Sources* 157 (2006) 11-27.
- [17] J.-M. Tarascon, M. Armand, *Nature* 414 (2001) 359-367.
- [18] M. Galiński, A. Lewandowski, I. Stępniański, *Electrochimica Acta* 51 (2006) 5567-5580.
- [19] C.A. Angell, W. Xu, M. Yoshizawa, A. Hayashi, J.-P. Belieres, P. Lucas, M. Videa, in: H. Ohno (Ed.), *Electrochemical Aspects of Ionic Liquids*, first ed., Wiley-Interscience, Hoboken, New Jersey, 2005 (Chapter 2).
- [20] J.S. Wilkes, J.A. Levisky, R.A. Wilson, C.L. Hussey, *Inorganic Chemistry* 21 (1982) 1263-1264.
- [21] Y. Hou, Y. Gu, S. Zhang, F. Yang, H. Ding, Y. Shan, *Journal of Molecular Liquids* 143 (2008) 154-159.
- [22] H. Every, A.G. Bishop, M. Forsyth, D.R. MacFarlane, *Electrochimica Acta* 45 (2000) 1279-1284.
- [23] M. Kunze, S. Jeong, E. Paillard, M. Winter, S. Passerini, *Journal of Physical Chemistry C* 114 (2010) 12364-12369.
- [24] W.A. Henderson, S. Passerini, *Chemistry of Materials* 16 (2004) 2881-2885.
- [25] Q. Zhou, P.D. Boyle, L. Malpezzi, A. Mele, J.-H. Shin, S. Passerini, W.A. Henderson, *Chemistry of Materials* 23 (2011) 4331-4337.
- [26] K. Kubota, T. Nohira, T. Goto, R. Hagiwara, *Electrochemistry Communications* 10 (2008) 1886-1888.

- [27] R. Lin, P.-L. Taberna, S. Fantini, V. Presser, C.R. Pérez, F. Malbosc, N.L. Rupasinghe, K.B.K. Teo, Y. Gogotsi, P. Simon, *Journal of Physical Chemistry Letters* 2 (2011) 2396-2401.
- [28] R.P. Swatloski, J.D. Holbrey, R.D. Rogers, *Green Chemistry* 5 (2003) 361-363.
- [29] S.I. Lall, D. Mancheno, S. Castro, V. Behaj, J.I. Cohen, R. Engel, *Chemical Communications* 24 (2000) 2413-2414.
- [30] L. Gubicza, N. Nemestothy, T. Frater, K. Belafi-Bako, *Green Chemistry* 5 (2003) 236-239.
- [31] C. Villagran, M. Deetlefs, W.R. Pitner, C. Hardacre, *Analytical Chemistry* 76 (2004) 2118-2123.
- [32] R.J. Bernot, M.A. Brueseke, M.A. Evans-White, G.A. Lamberti, *Environmental Toxicology and Chemistry* 24 (2005) 87-92.
- [33] C. Arbizzani, M. Biso, D. Cericola, M. Lazzari, F. Soavi, M. Mastragostino, *Journal of Power Sources* 185 (2008) 1575-1579.
- [34] C. Largeot, C. Portet, J. Chmiola, P.-L. Taberna, Y. Gogotsi, P. Simon, *Journal of the American Chemical Society* 130 (2008) 2730-2731.
- [35] N. Handa, T. Sugimoto, M. Yamagata, M. Kikuta, M. Kono, M. Ishikawa, *Journal of Power Sources* 185 (2008) 1585-1588.
- [36] M. Kunze, M. Montanino, G.B. Appetecchi, S. Jeong, M. Schonhoff, M. Winter, S. Passerini, *Journal of Physical Chemistry A* 114 (2010) 1776-1782.
- [37] P. Wasserscheid, T. Welton, *Ionic Liquids*, in *Synthesis*, second ed., WILEY-VCH, Weinheim, 2008.
- [38] Y. Zhu, S. Murali, M.D. Stoller, K.J. Ganesh, W. Cai, P.J. Ferreira, A. Pirkle, R.M. Wallace, K.A. Cychoz, M. Thommes, D. Su, E.A. Stach, R.S. Ruoff, *Science* 332 (2011) 1537-1541.
- [39] S. Brunauer, P.H. Emmett, E. Teller, *Journal of the American Chemical Society* 60 (1938) 309-319.
- [40] Y. Zhu, S. Murali, M.D. Stoller, A. Velamakanni, R.D. Piner, R.S. Ruoff, *Carbon* 48 (2010) 2118-2122.
- [41] R. Lin, P.-L. Taberna, J. Chmiola, D. Guay, Y. Gogotsi, P. Simon, *Journal of the Electrochemical Society* 156 (2009) A7-A12.
- [42] L.L. Zhang, R. Zhou, X.S. Zhao, *Journal of Materials Chemistry* 20 (2010) 5983-5992.
- [43] R. Kötz, M. Hahn, R. Gallay, *Journal of Power Sources* 154 (2006) 550-555.
- [44] H. Kurig, A. Janes, E. Lust, *Journal of the Electrochemical Society* 157 (2010) A272-A279.
- [45] V. Ruiz, T. Huynh, S.R. Sivakumar, A.G. Pandolfo, *RSC Advances* 2 (2012) 5591-5598.
- [46] C. Largeot, P.L. Taberna, Y. Gogotsi, P. Simon, *Electrochemical and Solid-State Letters* 14 (2011) A174-A176.
- [47] E. Iwama, P.L. Taberna, P. Azais, L. Brégeon, P. Simon, *Journal of Power Sources* 219 (2012) 235-239.
- [48] NASA technical reports sever. <<http://naca.larc.nasa.gov/search.jsp?R=20100001352&qs=N%3D4294964234%2B4294943931%2B4294350901>>.
- [49] J. Reiter, J. Vondrak, J. Michalek, Z. Micka, *Electrochimica Acta* 52 (2006) 1398-1408.
- [50] E.J. Brandon, W.C. West, M.C. Smart, L.D. Whitcanack, G.A. Plett, *Journal of Power Sources* 170 (2007) 225-232.
- [51] A.-K. Hjelm, T. Eriksson, G. Lindbergh, *Electrochimica Acta* 48 (2002) 171-179.
- [52] A. Izadi-Najafabadi, S. Yasuda, K. Kobashi, T. Yamada, D.N. Futaba, H. Hatori, M. Yumura, S. Iijima, K. Hata, *Advanced Materials* 22 (2010) E235-E241.
- [53] T. Kyotani, J. Chmiola, Y. Gogotsi, in: F. Beguin, E. Frackowiak (Eds.), *Carbon Materials for Electrochemical Energy Storage Systems*, CRC Press/Taylor and Francis, Boca Raton, FL, 2009.



Her research is focused on EQCM study of ion adsorption at nanoporous carbon electrode for supercapacitor application.

Wan-Yu Tsai received her B.S. in Materials Science and Engineering from National TsingHua University in Taiwan in 2008. Being awarded the Erasmus Mundus Scholarship, she joined the MESC (Materials for Energy Storage and Conversion) master program in 2009, and received her M.S in 2011. She is currently a PhD student in Paul Sabatier University (Toulouse, France), under Professor Simon and Professor Taberna's guidance.



SOLVIONIC. She is currently on a postdoctoral research position under the leadership of Professor Simon. Research includes electrochemical studies of electrolytes (ionic liquids and mixtures) and electrode materials for supercapacitors and batteries.

Rongying Lin was conferred a Bachelor of Applied Science in Materials Chemistry from the National University of Singapore (NUS) in 2004. She worked as a research assistant in NUS for one year before being awarded the Erasmus Mundus scholarship for MESC master program from 2006 to 2008. In 2012, she received her Ph.D. in Materials Science from the University of Paul Sabatier (France), achieved through industrial collaboration with



studying the reduction of exfoliated graphite oxide, and energy storage in systems with graphene-based materials as the electrodes.



Ruoff's group as a postdoctoral research fellow at The University of Texas at Austin. Dr. Zhang's research interest is developing high-performance energy storage materials and systems.

Dr. Li Li Zhang received her B. Eng. in Chemical and Biomolecular Engineering from the National University of Singapore in 2004. After two years industrial experiences in Micron, she continued her Ph.D. study in the same department at the National University of Singapore from 2006 and received her Ph. D degree in 2011. She worked as a research engineer from 2010 to 2011 at NUS and now she works in Professor



John serves as the president of the MRS chapter at Drexel and is also highly involved in the local ECS and ASM chapters.



Rodney S. Ruoff joined The University of Texas at Austin as a Cockrell Family Regents endowed chair in September, 2007. His Ph.D. is in Chemical Physics from the University of Illinois-Urbana (1988) and he was a Fulbright Fellow in 1988-89 at the Max Planck Institute fuer Stroemungsforschung in Germany. He was the John Evans Professor of Nanoengineering at Northwestern University and director of NU's Biologically

Inspired Materials Institute from 2002-2007. He has co-authored 330 peer-reviewed publications devoted to materials science, chemistry, physics, mechanics, engineering, and biomedical science. He is a Fellow of the APS and the AAAS.



Patrice Simon obtained his PhD in 1995 in Material Science at Ecole Nationale-Supérieure de Chimie de Toulouse. He joined the Conservatoire National des Arts et Métiers in Paris in 1996 as Assistant Professor and moved to Université Paul Sabatier in 2001, where he is currently Professor of Material Science. He holds a Chair of Excellence of the EADS Foundation and was awarded in 2011 with an Advanced

Grant from the European Research Council (ERC, Ionaces project). His research is focused on the synthesis and characterization of nanostructured materials for electrochemical capacitors and Li-ion batteries.



Pierre-Louis Taberna is a CNRS researcher at the CIRIMAT UMR 5085 - Université de Toulouse III, France. He has been working for more than ten years on the study and the modification of interfaces for energy storage materials. The aim of his work is mainly to nano-architect electrodes both for supercapacitors and lithium ion batteries. Along with performance enhancement it is aimed also to achieve a better understanding of charge storage mechanisms.



Dr. Yury Gogotsi is Distinguished University Professor and Trustee Chair of Materials Science and Engineering at Drexel University. He also serves as Director of the A.J. Drexel Nanotechnology Institute. His Ph.D. is in Physical Chemistry from Kiev Polytechnic and D.Sc. in Materials Engineering from the Ukrainian Academy of Sciences. His research group works on nanostructured carbons and other nanomaterials. He has

co-authored more than 300 journal papers. He is a Fellow of AAAS, MRS, ECS and ACerS and a member of the World Academy of Ceramics.